

FORM-FACTOR FOR A TARGET USED FOR POSITRONS GENERATION WITH UNDULATOR RADIATION CONVERSION¹

A. Mikhailichenko

Cornell University, LEPP, Ithaca NY 14853

It is shown here that the needle type target gives advantages in conversion of gammas from helical undulator into positrons. This is not possible with usual electron to positron production method.

INTRODUCTION

In all operational electron-positron colliders, positrons created by primary electrons in a heavy material target. This primary electron beam with energy E_0 , when hits the target, develops a cascade, what is a mixture of electrons, positrons and gammas. Namely these gammas are responsible for positron creation in electric field of nucleus of target material. This cascade develops along the target starting from the points of penetration of initial beam. The cascade propagates inside matter until energy of particles reaches the critical value, $E_c \cong 610 / (Z + 1.24)$, MeV, Z stands for atomic number. Transverse size of the cascade in maximum is of the order of Molière radius $R_M \cong X_0 E_s / E_c$, where X_0 is a radiation length, $E_s = \sqrt{4\pi\alpha} \cdot mc^2 \cong 21.2 \text{ MeV}$ – is a scale energy. Naturally, the Molière radius, expressed in cm, is bigger for lighter materials, as $R_M \approx 0.035 \cdot Z \cdot X_0$ and $X_0 \propto A / Z^2$, so $R_M \propto A / Z$, where A is atomic weight. For W with its $Z=74$, $R_M^W \cong 2.57 X_0$ ($l_M^W = 0.9 \text{ cm}$), as geometrical length corresponding to the radiation one is $l_{X_0} \cong 0.35 \text{ cm}$. For Ti, with its $Z=22$, $R_M^{Ti} \cong 0.7 X_0$ ($l_M^{Ti} = 2.45 \text{ cm}$), as $l_{X_0} \cong 3.55 \text{ cm}$. Cascade reaches its maximum at the depth $t_{max} \cong X_0 \ln(E_0 / E_c) / \ln 2$ with the number of the particles there about $N_{max} \cong E_0 / E_c$. So one can estimate geometrical volume occupied by cascade as

$$V_c \cong \frac{\pi}{3} l_{t_{max}} l_M^2 \cong \frac{\pi}{3 \cdot \ln 2} l_{X_0}^3 \left(\frac{E_s}{E_c} \right)^2 \ln \frac{E_0}{E_c} \propto l_{X_0}^3 \cdot Z^2 \propto A^3 / Z^4. \quad (1)$$

The ratio of these volumes for Tungsten and for Titanium goes to be

$$V_c^{Ti} / V_c^W \propto \left(\frac{l_{X_0}^{Ti}}{l_{X_0}^W} \right)^3 \times \left(\frac{Z^{Ti}}{Z^W} \right)^2 = \left(\frac{3.55}{0.35} \right)^3 \times \left(\frac{22}{74} \right)^2 \approx 88, \text{ i.e. the volume involved in cascade inside}$$

Ti is about 88 times the volume inside W for the same initial energy of primary electrons. The number of particles in cascade for W will be ~ 3.4 times bigger than in Ti. Of course, this is estimation only, and gives qualitative numbers; accurate calculation needs to be carried numerically.

In many laboratories, including BINP Novosibirsk, there were carried investigations on how shape of the target can increase the yield of positrons. Idea is illustrated in Fig. 1. Desire was to let positrons, created inside initial parts of volume, escape from the target through the sides without experience of multiple scattering.

¹ Electronic version is available at http://www.lns.cornell.edu/public/CBN/2003/CBN03-2/CBN03_2.pdf

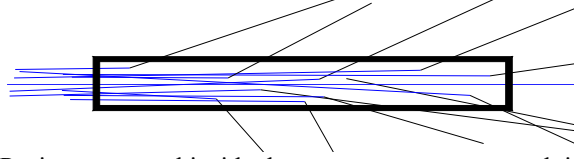


FIGURE 1: Positrons created inside the target can escape trough its sides.

Result for W in traditional conversion scheme was negative, however– targets are relatively short and there is no much room for manifestation of angular escape. So, now all operational targets can be treated as wide ones –they are wider, than the width of a cascade at maximum, $R_t \geq R_M$.

POSITRONS GENERATION WITH UNDULATOR

Method of polarized positron generation was proposed in [1]. In this new method, at first stage, circularly polarized gammas obtained from primary high-energy (>100 GeV) electron/positron beam by beamstrahlung in a helical undulator/wiggler. At second stage these circularly polarized gammas converted into positrons/electrons into thin, $\sim 0.5X_0$, target. Just selecting the positrons or electrons with highest possible energy, one can obtain a beam of *longitudinally polarized* secondary particles. For the wiggling by primary beam it was suggested to use electromagnetic waves, fields of helical crystals and static helical fields [1]. Static helical magnetic fields were found as the only practical ones, however.

Polarized positrons and electrons were immediately included in general scheme of VLEPP. In addition to polarization, the scheme drastically, ≥ 100 times, reduces the heat deposition in a target.

Laser radiation as a kind of electromagnetic wave was specially mentioned in 1992 [2] as an example. Formulas and the method are the same, naturally. Later, in 1995, the way with laser radiation was manifested as a direct line for JLC [3,4].

For successful operation, the number of periods in undulator must be around $M \cong 10^4$, what defines the total length of undulator $L = M\lambda_u \geq 100$ m with period $\lambda_u \cong 1$ cm. This covers the losses associated with energy selection of particles. It was found (see [7, 9] for details) that optimal value of undulatority factor $K = eH\lambda_u / 2\pi mc^2$ is $K \sim 0.4$. Polarization $\geq 65\%$ can be obtained with such long undulator.

So one can see, that any percentage in increase of positron production allows the same percentage in cut of 100 m undulator.

Now let us estimate possible gamma spot size σ_γ on the target and compare it with R_M . This will require for proper choice of the target diameter. Angular spread of radiation is

$$\langle \vartheta^2 \rangle \cong \begin{cases} \frac{\gamma\mathcal{E}}{\gamma\beta} + \frac{1+K^2}{\gamma^2} \\ \frac{\gamma\mathcal{E} + \delta}{\gamma\beta} + \frac{1+K^2}{\gamma^2} \end{cases}, \quad (2)$$

where upper part applies to situation, when undulator installed a prior to IP, the lower part applies to post IP location of undulator. Here δ describes emittance dilution, $\beta \cong L$ is envelope function at location of undulator, $\gamma = E / mc^2$ is relativistic factor. The unperturbed emittance is typically $\gamma\mathcal{E}_x \sim 3 \cdot 10^{-6} m \cdot rad$, so first term goes to $\frac{\gamma\mathcal{E}}{\gamma\beta} = 10^{-13}$ for $\beta \cong L$ and $E_0 \cong 150$ GeV

($\gamma \cong 3 \cdot 10^5$) primary beam. Second term yields $(1 + K^2) / \gamma^2 \cong 10^{-11}$ so it is dominant and gives angle RMS $\sqrt{\langle \vartheta^2 \rangle} \cong 3.16 \cdot 10^{-6}$. If the undulator installed after IP, then dilution is playing a role. The last one can be estimated as RMS of angular kick spread $\Delta\vartheta$. Usually for flat beam at IP with $\sigma_x \geq \sigma_y$, magnetic field has one dominant component, $H_x \cong \frac{eNc}{\sigma_x \sigma_s} \frac{y}{\sigma_y}$, (all parameters taken at IP) which yields the angular kick spread square with amplitude

$$\langle \Delta\vartheta_d^2 \rangle \cong \left(\frac{\Delta p_y}{p} \right)^2 = \left(\frac{eH_x \Delta t}{p} \right)^2 \cong \left(\frac{r_0 N}{\gamma \sigma_x} \right)^2, \quad (3)$$

where $\Delta t \cong \sigma_s / c$. Substitute $N \cong 10^{10}$, $\sigma_x \cong 250 \text{ nm}$ in (3), one can obtain $\langle \Delta\vartheta_d^2 \rangle \cong 1.4 \cdot 10^{-7}$. The last yields emittance dilution as big as $\delta \cong \gamma \beta_y \cdot \langle \vartheta_d^2 \rangle \cong 4.2 \cdot 10^{-6} \text{ m} \cdot \text{rad}$ for $\beta_y \cong \sigma_s \cong 100 \mu\text{m}$, i.e. roughly the same as for horizontal direction and it does not affect RMS angle estimation practically. So the size of the gamma beam and angular spread go

$$\begin{aligned} \sigma_\gamma &\cong \sqrt{\gamma \varepsilon \beta / \gamma + D \sqrt{\langle \vartheta^2 \rangle}} \cong L \sqrt{\langle \vartheta^2 \rangle} \cong 5 \cdot 10^{-4} \text{ m}, \\ \sigma'_\gamma &\cong \sqrt{\langle \vartheta^2 \rangle} \cong 5 \cdot 10^{-6}, \end{aligned} \quad (4)$$

where the distance from the target to the undulator D estimated as $D \sim L$ and the size of primary electron/positron beam included too. These numbers used for numerical modeling of conversion.

DESCRIPTION OF PROCEDURE

For calculations the code CONVER [5] operating on PC was used. The code, in its turn, uses results of calculations done by other code- UNIMOD2 [6]. The last one, EGS-like code, calculates the cascade processes in semi-infinite media, keeping the individual history of every particle in cascade since the first appearance. Calculations in CONVER arranged so that the files obtained from UNIMOD2 are transferred to PC and user can easily assemble a target of any shape as a sum of isles, each of them is a body of revolution with polygonal cross section. If trajectory of any particle in cascade meets empty space, its trajectory just continued linearly by CONVER up to the next isle with material. So, basically all process looks like one in infinite media and if insertions with empty spaces met, then trajectories just going straight. Files from EGS code can be used as initial ones for CONVER as well. In code one can insert angular spread and size of initial gamma-beam. Operating on PC with large file with results obtained from UNIMOD2 on big machine drastically increases productivity of calculations. Individual parameters of every particle in cascade at the out of target region allow to calculate efficiency as well as to prepare the files for further tracking.

As it was mentioned, the files containing the cascade history for chosen material of target (W and Ti in our case) must be obtained in separate run with UNIMOD2. Once obtained, these files can be used for calculations with target of any shape. Special files were prepared for W and Ti targets for 10, 15, 20, 25, 30 and 40 MeV primary gamma beam [7]. All these files (except one for 25 MeV in Ti) do not keep positron if its energy is less than half of energy of gamma quanta. This done for the purposes of shortening the file length as positrons in any case selected by the threshold, which is half of maximal possible, i.e. $E_{th} = (E_\gamma - 2mc^2) / 2$. The files prepared allowed calculations both for W and Ti target of any shape. The shape of the target was

investigated for W target only, however. Tungsten was found acceptable from any point of view for the program of linear collider at that time. For Ti target calculations done for infinitely wide target. Results from CONVER written to the file were used for the following processing with other numerical codes (RRED and OBRA). These codes in it's turn prepare also the file, every row of each has the following format: first number is the positron number, second stands for the number of processed photons, third –the positron's initial energy; next three–are 3D out-coordinates, following three numbers strand for projections of unit vector $\vec{n} = \vec{p}/|p|$ to the axes; the next number is the energy of positron at the moment of creation; next number- is generation and the last one-x coordinate of point, when positron created. Basically the last 10 numbers are transferred from CONVER output file.

With help of these last codes numerous parameters were calculated, such as, for example, polarization, energy deposition and efficiency as function of thickness, see Fig.2 [7]. It was found for wide W target, that the efficiency of positron conversion, calculated as a ratio of total number of photons to the number of positrons in desirable angle and energy spectrum could reach 6.5% for $E_\gamma \cong 40MeV$ and capturing angle $\pm 0.5rad$.

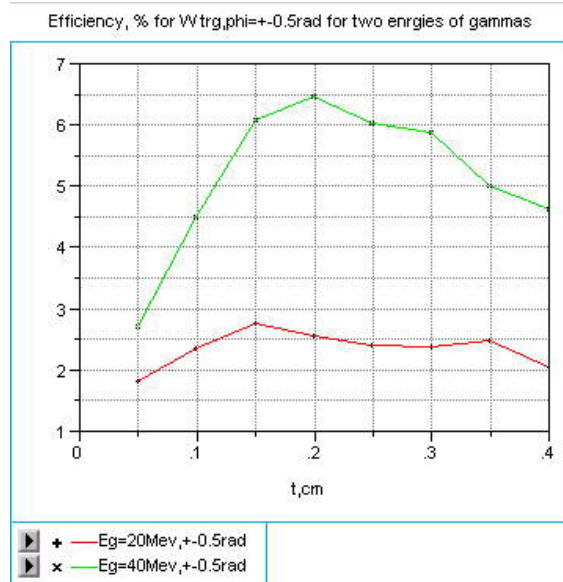


FIGURE 2: (Color) Efficiency as functions of thickness for W target. Energy of gammas $E_\gamma=20MeV$ and $E_\gamma=40MeV$.

Thickness of W target which gives maximum yield was found to be about 0.2 cm. For W target it was found that average energy deposition at the end of the target was 250 MeV/g. This deposition yields the heating $\Delta T \cong 2.93 \cdot 10^{-10}$ def/photon. As one can see from Fig.2 for primary energy of gammas 20 MeV, required number of photons for efficiency normalized to each initial electron in undulator ~ 1 it is necessary to have ~ 40 photons from undulator, so the heating will be $\Delta T \cong 2.93 \cdot 10^{-10} \times 39 \cong 1.14 \cdot 10^{-8}$ deg/ e^+ . This will bring the temperature gain of end side of the target of the order 114 deg for the beam with 10^{10} positrons in the bunch. For 40 MeV photons, only ~ 15 photons required, so the temperature gain will be $\Delta T \cong 45$ deg per pulse.

TI TARGET

Although utilization of undulator/wiggler conversion decreases average power deposition in target $>10^2$ times, it is still not enough for TESLA. Utilization of Ti for target was suggested in [8]; namely this publication initiated work with Ti in [7]. In addition to bigger volume of cascade developing in this material, it has higher heat capacity. This is a sequence of Dulong–Petite law. Really, intrinsic energy of media is $Q \cong \frac{3}{2}k_B N_A T + rotation \approx 3k_B N_A T$, where $k_B \cong 1.38 \times 10^{-23} \text{ Joules}/^\circ K$ –is the Boltzmann’s constant and $N_A \cong 6.022 \cdot 10^{23} \text{ mol}^{-1}$ is the Avogadro's constant. Heat capacity goes to be $c_p \cong \partial Q / \partial T = 3k_B N_A \approx 25 \text{ Joule}/\text{moll}/^\circ K$ and one can see, that for Ti heat capacity is about 184/48~4times bigger.

Efficiency for Ti target as functions of thickness are represented in Fig. 3. This figure will serve as a reference one for comparison of shapes. For wide Ti target the efficiency found to be ~2.7%, 1.7% and 1.25% for the primary gamma beam with $E_0 = 30 \text{ MeV}$, 20MeV and 10MeV respectively.

Now, as the cascade process is no longer involved in conversion with undulator, result of shape optimization might indicate some significant improvements. First results were quite positive. This was mentioned for the first time in [9]. For the target with Length/diameter ratio ≈ 10 , for $E_\gamma = 20 \text{ MeV}$ efficiency was found to be $\approx 2.67\%$ for target of 4cm long $\sigma_\gamma \cong 0.1 \text{ cm}$, diameter of target is 0.4cm. This needs to be compared with 1.7% for infinitely wide target.

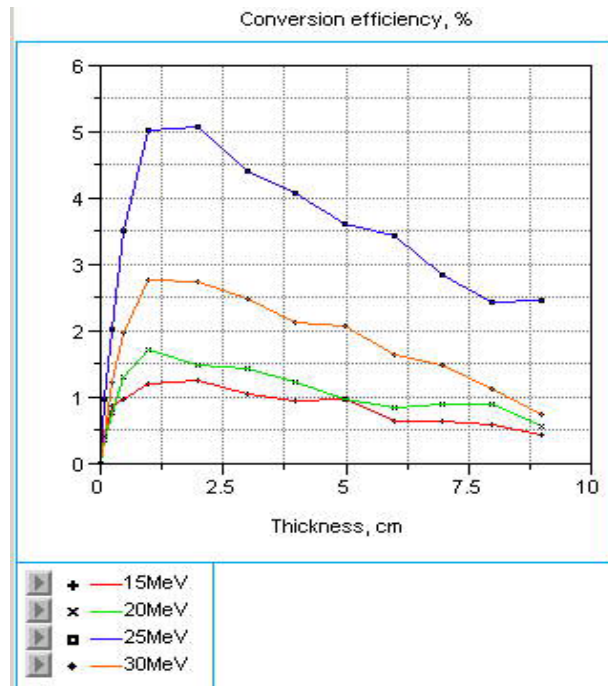


FIGURE 3: (Color) Efficiency as a function of the thickness for wide Ti target, %. Top curve for gammas 25 MeV in full energy spectrum. This might be interesting for unpolarized positron generation. Angle (polar) of capture is $\Delta\vartheta = \pm 0.5$ rad. All other curves represent the upper half of energy spectrum. Statistical error is about 10% for each curve.

As all the files with Ti from UNIMOD2 were preserved since the [7] done, it was easy to make calculations for the form-factor now. As it was mentioned, CONVER also allows seeing trajectory of each individual particle in the cascade. Special key allows select the type of

particles to be visualized. Example of graphical presentation of output coordinates is shown in Fig. 4 and Fig.5. Here the shape of cylinder is clearly visible. Each point represents coordinates, when particle (positron) leaves the target. So these are the points when trajectories puncture the surface of the target. As it was mentioned, each of these points accompanied by direction of motion, final energy and energy and coordinate when created.

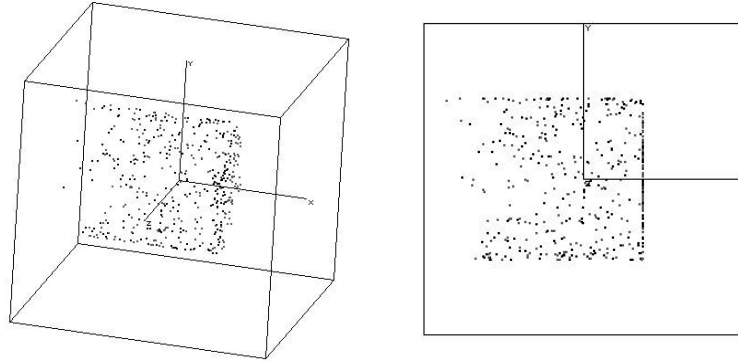


FIGURE 4: Coordinates of positrons leaving cylindrical target. All positrons represent the upper half of energy spectrum. At the right the side view of the picture at left is shown. Diameter of cylinder is 0.5mm, Length of the target is 2 cm. Efficiency is this example is 4.63%, $E_\gamma = 30\text{MeV}$. Length is not in scale.

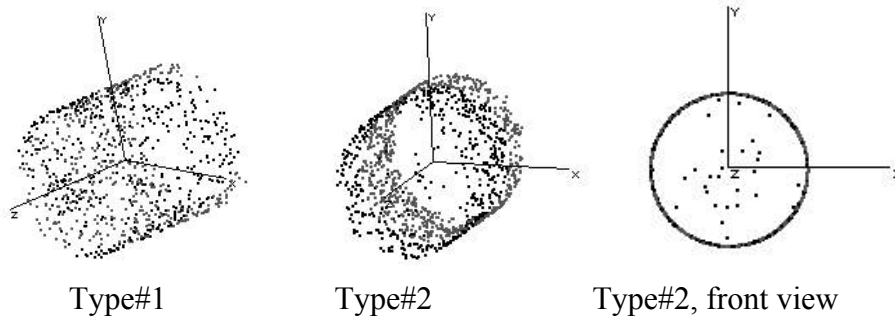


FIGURE 5: A different type of arrays of output coordinates. Type#1 for relatively short target. For the long target mostly of trajectories escape through the sidewalls of cylinder, type #2. Lengths of cylinders are not in scale with diameter.

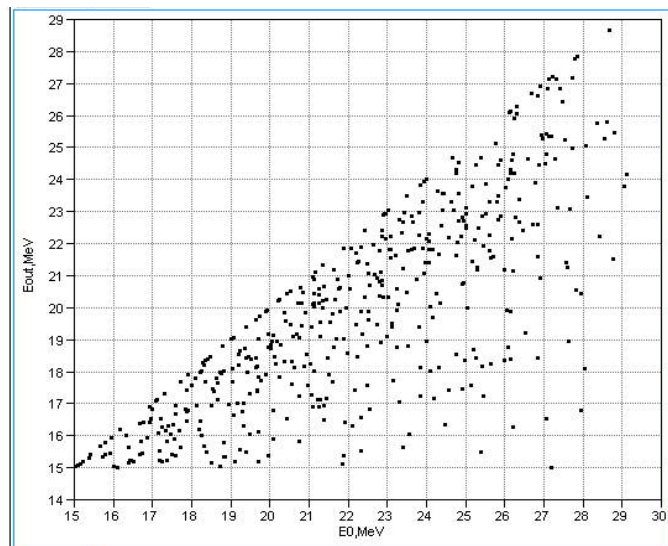


FIGURE 6: Typical correlation between energy at the moment of creation and at the out. All positrons represent the upper half of energy spectrum. Initial energy of quantas $E_\gamma = 30\text{ MeV}$. Cylindrical target.

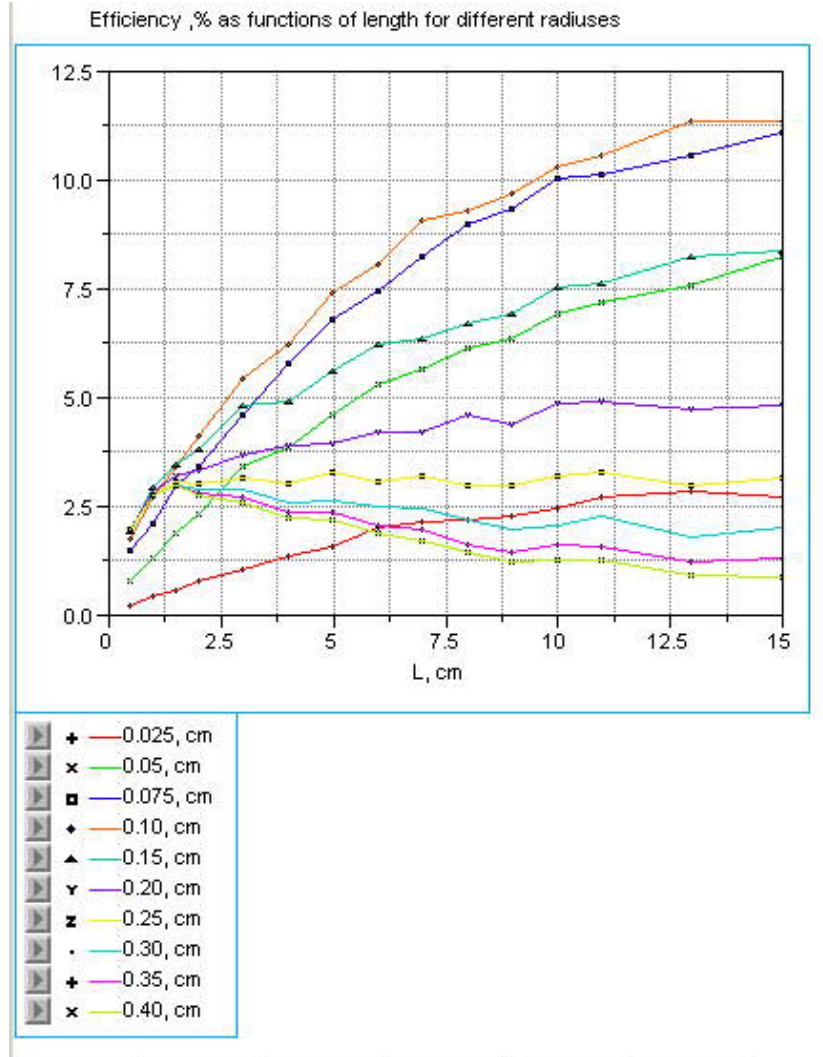


FIGURE 7: (Color) Efficiency as functions of target length for different values of radius.

In Fig.7 the efficiency represented as functions of thickness for different target diameter. Transverse size of gamma beam here was $\sigma_\gamma = 0.05\text{cm}$. Energy of photons $E_\gamma = 30\text{ MeV}$, positrons selected in interval 15-30 MeV within capturing polar angle $\Delta\vartheta \leq 0.5\text{ rad}$. It is visible from here that for targets with small radius, $R_t \leq 2\sigma_\gamma$, there is a monotonic growth of number of positrons coming out of target. After $R_t > 4\sigma_\gamma$ the graphs began decline as functions of thickness –positrons cannot escape freely though the sides. One can see, that efficiency of positron conversion for infinitely wide target has maximum around 1.25 cm long-target in agreement with Fig.3. Accuracy of calculation defined by the number of primary photons used for generation of cascade in UNIMOD2. This number was $\sim 10^4$, corresponding accuracy of calculation is $\leq 10\%$. Same data, as in Fig.7, but transposed, are represented in Fig.8. Typically parameters of targets considered for DESY so far located behind the right edge of this Fig.8-wide targets. It is clearly seen from this figure, that optimum target diameter is somewhere between 0.75-1.0 mm. Even for target having length $\sim 1\text{ cm}$ it is better to have its diameter small, something about 1 mm. This is a new result.

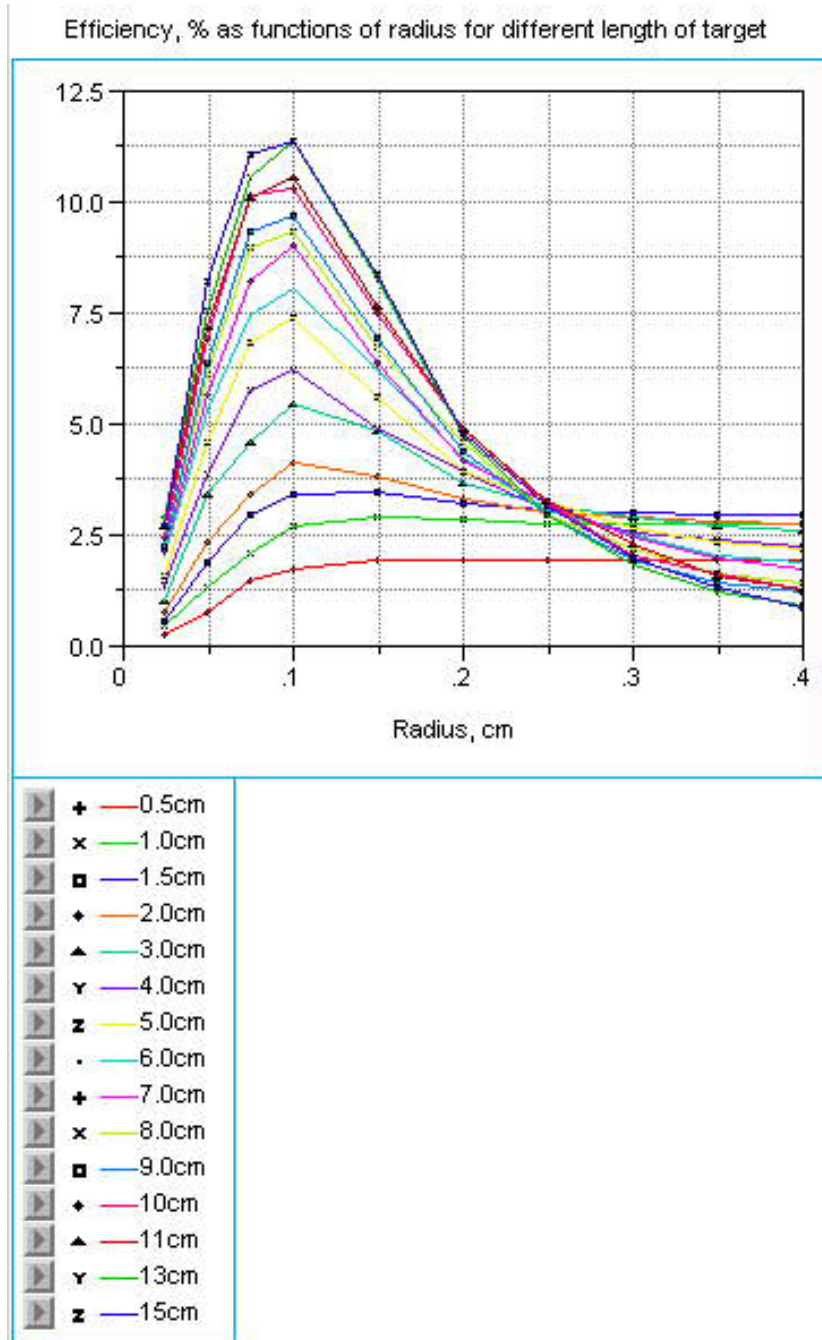


FIGURE 8: (Color) Efficiency as functions of target radius for fixed length. Basically this is the same data as in Fig.7, but transposed. Right now TESLA has a plan to work with a target which parameters selected from behind the right edge of this Figure, where $R_t \geq R_M$.

So the strategy in obtaining maximum yield is now to increase the length of the target simultaneously decreasing its radius to about $R_t \cong 2\sigma_\gamma$

TECHNICAL REALIZATION OF COLLECTION SYSTEM

Some complication of optics is that now the increased focal depth required, as positrons can escape now from any point along the target. That is the price for possible enhancement. However for targets with 1 cm long and 1 mm in diameter there is not difference at all. Although calculations with real focusing elements were not carried so far, let us describe some of these, keeping in mind to perform such calculations in a future. The files with initial data can be easily generated.

First scheme, Fig.9, uses short target with reduced diameter. Here Ti needles pressed into Be wheel. All assembly located in vacuum. Rotation of wheel synchronized with repetition rate of machine, so that next gamma-beam hits each time new target.

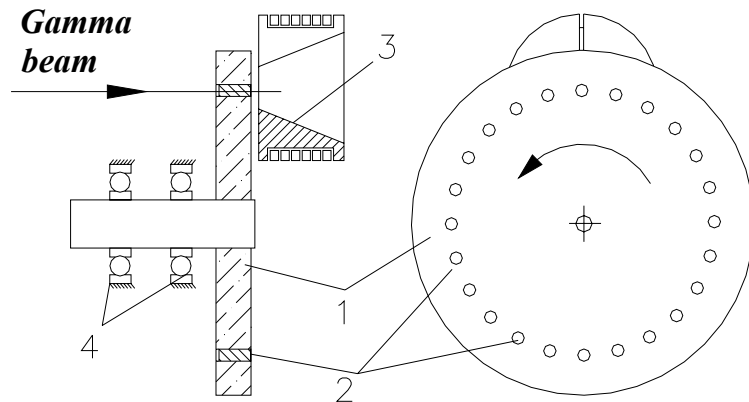


FIGURE 9: Realization of multi-target assembly. Ti needles pressed into Beryllium wheel. Here 1 is Beryllium wheel, 2 are Ti needles, 3—is a flux concentrator, and 4—bearings.

Total power deposited in the target system is few hundreds Watts only, so the problem of cooling is relaxed drastically. A lot of technical solutions for this problem can be proposed immediately. Other technical solution, which can be used for long targets, is shown in Fig.10. Here the target of 2-6 cm long enclosed into a Ti cylinder with a coolant running inside. For coolant it is naturally to use liquid Lithium. As melting temperature for Lithium is 180.54°C only, it is not a problem to arrange a system for proper cooling. For pumping of liquid Lithium a well-developed technique can be used [10].

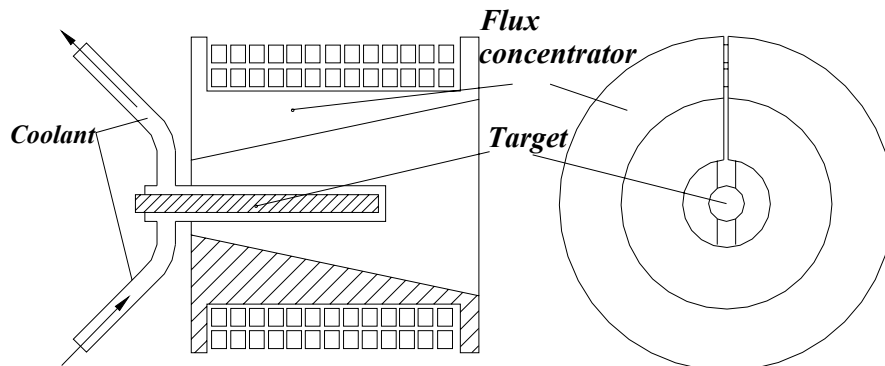


FIGURE 10: Another technical realization of target assembly. Ti target enclosed in Ti container with Li coolant.

Positrons escaped though the sides extracted outside the flux concentrator. Some of positrons can hit the target again, but as the target is thin in transverse direction, one may expect that the scattering will not kill the positron. This scheme is working for short targets too.

Scheme with flux concentrator of this type was successfully implemented into CESR [11].

Possible solution for very long and, hence, thin target, with length ≥ 6 cm and ~ 0.3 - 0.5 mm in radius is shown in Fig.11. Here the Ti alloy wire just stretched between to v-pulleys and moved with constant linear speed. These pulleys made from Beryllium, which eliminates energy deposition and scattering. Cooling arranged outside the flux concentrator. The wire can be arranged as a loop as well as winding onto two spools, one at each side.

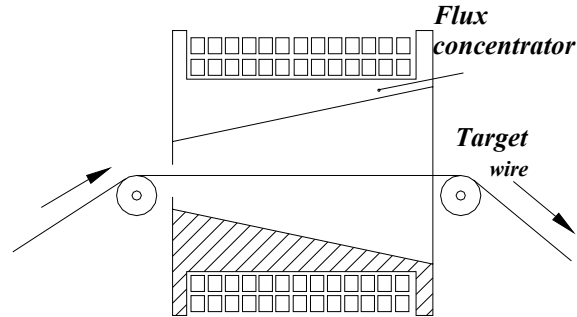


FIGURE 11: Another technical realization of target assembly. Ti alloy wire runs on Be V-pulleys and cooled outside of flux concentrator.

One other way to increase cooling of target is shown in Fig. 12. Coolant flowing between discs effectively working because the distance from coolant edge to the point inside the target defined by thickness of the disc, not a diameter.

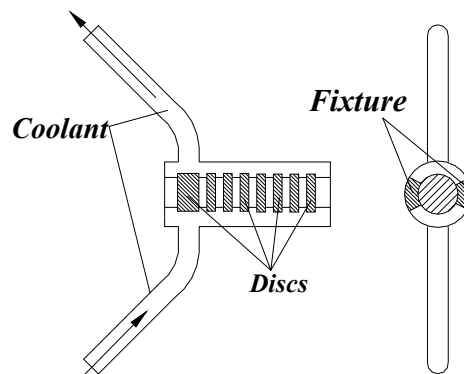


FIGURE 12: Sandwich-type high power target. W or Ti target discs enclosed in Ti container with coolant.

Let us say here without much consideration, that a suspension of W powder in liquid Li or In-Ga mixture can be considered as extreme media for target.

One other way to increase positron production –utilization of few targets and combining positrons into longitudinal phase-space is among guaranteed ones [1, 7, 9, 12]. This is also some kind of form-factor problem.

CONCLUSION

Increase in positron production allows proportional shortage of ~ 100 -meter undulator and/or a source of additional operational margins for conversion system.

It is shown here for the first time, that needle-like Ti target with radius $\sim 1\text{mm}$ ($R_t \cong 2\sigma_\gamma$) can give yield $\sim 11.4\%$, which needs to be compared with $\sim 2.7\%$ yield for infinitely wide target and the same capturing angle $\sim 0.5\text{rad}$ and for $E_\gamma = 30\text{MeV}$. This is two times bigger than for W target. Of course final numbers will depend on capturing system, however indication, that form-factor can improve the yield so much, gives the basis for target optimization for real LC conversion unit. Decreasing diameter of the target also helps in cooling, even if the target is short.

Optimistically speaking, one can expect shortage of undulator length at least in half if the optimal target shape is used. If the length kept the same, this optimization will give wider operational margins or higher polarization, as one can select among much more positrons now.

In conclusion Author thanks A.D. Bukin for permission to use his code, which made this job possible.

REFERENCES

- [1] V.E. Balakin, A.A. Mikhailichenko, *Conversion system for obtaining highly polarized electrons and positrons*, Preprint INP 79-85, Novosibirsk 1979.
- [2] E.G. Bessonov, *Some aspects of the theory and technology of the conversion systems of linear Colliders*, 15th International Conference on High Energy Accelerators, Hamburg, 1992, p.138.
- [3] T. Hirose, in *Proceedings of International Workshop on Physics and experiments with Linear Colliders*, Morioka, Iwate, Japan, September 8-12, 1995, World Science, Singapore, 1996, pp.748-756.
- [4] T. Okugi, et al., *Jpn. J. Apl. Phys.* 35 (1996) 3677.
- [5] A.D. Bukin, *Search of the optimum form of positron converter*, Preprint INP 90-100, Novosibirsk 1990.
- [6] A.D. Bukin, N.A. Grozina, M.S. Dubrovin e.a., UNIMOD2-Universal Simulating program for e^+e^- experiments, Manual, Preprint BINP 90-93, Novosibirsk 1990.
- [7] A.D. Bukin, A.A. Mikhailichenko, *Optimized Target Strategy for Polarized Electrons and Positrons Production for Linear Collider*, Budker INP 92-76, Novosibirsk, 1992.
- [8] J.Rossbach, K. Floetmann, *A High Intensity Positron source for Linear Collider*, DESY M-91-11.
- [9] A.A. Mikhailichenko, *Use of undulators at High Energy to Produce Polarized Positrons and Electrons*, Workshop on New Kinds of Positron Sources for Linear Colliders, SLAC, March 4-7, 1997, SLAC-R-502, pp. 229-284.
- [10] G.I. Silvestrov, *Liquid metal Targets for Intensive High-Energy Physics Beams*, *ibid*, p.376-407.
- [11] J. Barley, V. Medjidzade, A. Mikhailichenko, *New Positron source for CESR*, CBN 02-*
- [12] A. Mikhailichenko, *Conversion System for obtaining Polarized Electrons and Positrons at High Energy*, Translation of Dissertation, CBN 02-13, Cornell, 2002.